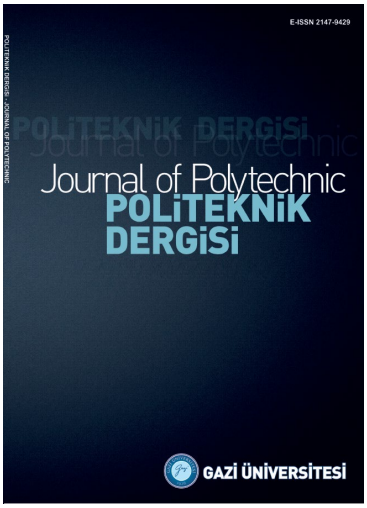

POLİTEKNİK DERGİSİ

JOURNAL of POLYTECHNIC

ISSN: 1302-0900 (PRINT), ISSN: 2147-9429 (ONLINE)
URL: http://dergipark.org.tr/politeknik

A swarm optimized ANN-based numerical treatment of nonlinear SEIR system based on zika virus.

Zika virüsü temelli doğrusal olmayan SEIR sisteminin sürüklenmiş yapay sinir ağı (ANN) tabanlı sayısal tedavisi.

***Yazar(lar) (Author(s))**: Farhad Muhammad Riaz[1], Junaid Ali Khan[2]*

ORCID[1]: 0000-0001-9167-8690

ORCID[2]: 0009-0004-0967-1211

To cite to this article: Riaz F. M., Khan J.A., "A Swarm Optimized ANN-based Numerical Treatment of Nonlinear SEIR System based on Zika Virus.", ***Journal of Polytechnic***, 28(5): 1349-1363, (2025).

Bu makaleye şu şekilde atıfta bulunabilirsiniz: Riaz F. M., Khan J.A., "A Swarm Optimized ANN-based Numerical Treatment of Nonlinear SEIR System based on Zika Virus.", ***Journal of Polytechnic***, 28(5): 1349-1363, (2025).

Erişim linki (To link to this article): http://dergipark.org.tr/politeknik/archive

DOI: 10.2339/politeknik.1543179

A Swarm Optimized ANN-based Numerical Treatment of Nonlinear SEIR System based on Zika Virus

Highlights

- *The Mexican Hat-Wavlevt-based ANN is employed to solve the nonlinear system of Zika virus Spread*
- *Error-based fitness function is demonstrated by using the system of differential equations*
- *Hybrid optimization scheme i.e. PSO-SQP is utilized to optimize the parameters of the neural designed neural network*
- *The correctness and stability of the scheme are analyzed through comprehensive statistical analysis*

Graphical Abstract

The computing efficiency of an artificial neural network is utilized to solve the Zika virus-based nonlinear differential system SEIR.

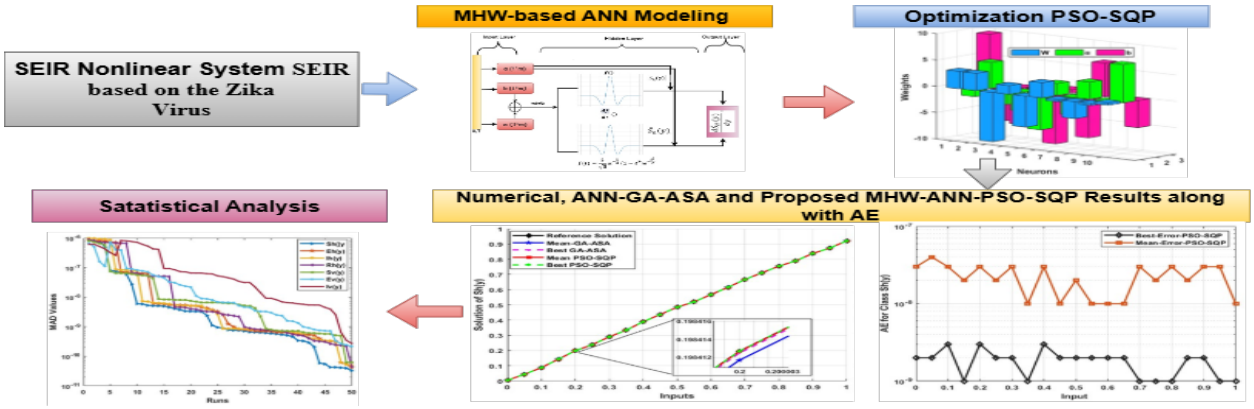

Figure. Flow chart of the Proposed MHW-ANN-PSO-SQP for SEIR based on Zika Virus.

Aim

The study aims to present a novel numerical method for solving a nonlinear SEIR model of the Zika virus using a hybrid computational framework.

Design & Methodology

The dynamics of Zika virus dissemination are examined using this model. The suggested framework solved the SEIR mathematical model by combining the ANN process with the swarm optimization process.

Originality

This study's novelty is a numerical analysis of the SEIR coupled nonlinear mathematical model based on Zika virus spread using the hybrid optimization process of global PSO and local search scheme SQP, as well as the computational efficiency of the Mexican Hat Wavlavt-based activation function

Findings

The suggested scheme's validity is indicated by the overlap solutions, and AE attests to its accuracy. The Min, Mean, and S.T.D. of the statistical operator are likewise within an acceptable range for solving the Zika virus spread-based SEIR nonlinear system.

Conclusion

Although the approximated solution of the proposed scheme is accurate, precise, and stable, the proposed scheme is reliable, however, due to the hybrid optimization procedure, the proposed scheme is computationally expensive.

Declaration of Ethical Standards

The author(s) of this article declares that the materials and methods used in this study do not require ethical committee permission and/or legal-special permission.

A Swarm Optimized ANN-based Numerical Treatment of Nonlinear SEIR System based on Zika Virus

Araştırma Makalesi / Research Article

Farhad Muhammad RİAZ[1], Junaid Ali KHAN[1*]

[1]Departement of Computer Science, HITEC University, Taxila, Pakistan

(Geliş/Received : 04.09.2024 ; Kabul/Accepted : 12.01.2025 ; Erken Görünüm/Early View : 17.02.2025)

ABSTRACT

The purpose of the current study is to present the numerical treatment of a nonlinear mathematical SEIR model based on the Zika virus using the Mexican Hat Wavelet-based feed-forward artificial neural network (MHW-ANN) together with the optimization scheme of global search, Particle Swarm Optimization (PSO) and local search Sequential Quadratic Programming (SQP), i.e. MHW-ANN-PSO-SQP. The Zika virus is an epidemic disease that can spread through the transmission of the virus known as Aedes, its model is based on susceptible-exposed-infected-recovered, i.e. SEIR that investigated the dynamics of virus spread. To solve the model an error-based fitness function is optimized through a hybrid computing scheme of MHW-ANN-PSO-SQP. To validate the precision, accuracy, stability, reliability, and computational complexity of the designed framework various cases have been taken for the virus. The results obtained from the MHW-ANN-PSO-SQP are compared to the well-known RK numerical solver and ANN-based (GA-ASA) to confirm the accuracy. At the same time, the absolute error validated the precision of the designed scheme. Additionally, the statistical analysis through different statistical operators is performed to validate the stability, convergence, and reliability of the MHW-ANN-PSO-SQP. Furthermore, the complexity of the presented scheme is analyzed through the Mean Execution Time (MET).

Keywords: SEIR mathematical model, Artificial neural network computation, swarming techniques, SQP, Mexican hat wavelet

Zika Virüsü Temelli Doğrusal Olmayan SEIR Sisteminin Sürüklenmiş Yapay Sinir Ağı (ANN) Tabanlı Sayısal Tedavisi

ÖZ

Mevcut çalışmanın amacı, Zika virüsü temelli doğrusal olmayan bir SEIR matematiksel modelinin sayısal çözümünü, Meksika Şapkası Dalga Dönüşümü (MHW) tabanlı ileri beslemeli yapay sinir ağı (ANN) ile birlikte, küresel arama optimizasyon şeması olan Parçacık Sürüsü Optimizasyonu (PSO) ve yerel arama olan Ardışık Kuadratik Programlama (SQP) kullanarak sunmaktır. Zika virüsü, Aedes adı verilen virüsün taşınması yoluyla yayılan bir salgın hastalıktır ve bu model, virüsün yayılma dinamiklerini inceleyen Susceptible-Exposed-Infected-Recovered yani SEIR temellidir. Modeli çözmek için, hata tabanlı bir fitness fonksiyonu, MHW-ANN-PSO-SQP hibrit hesaplama şeması ile optimize edilmiştir. Tasarlanan çerçevenin doğruluğunu, güvenilirliğini, stabilitesini, hassasiyetini ve hesaplama karmaşıklığını doğrulamak için, virüsle ilgili çeşitli durumlar incelenmiştir. MHW-ANN-PSO-SQP'den elde edilen sonuçlar, doğruluğu teyit etmek için iyi bilinen RK sayısal çözücü ve ANN tabanlı (GA-ASA) ile karşılaştırılmıştır. Aynı zamanda, mutlak hata, tasarlanan şemanın doğruluğunu doğrulamaktadır. Ayrıca, istatistiksel analiz, MHW-ANN-PSO-SQP'nin stabilitesini, yakınsamasını ve güvenilirliğini doğrulamak için farklı istatistiksel operatörler aracılığıyla yapılmıştır. Dahası, sunulan şemanın karmaşıklığı, Ortalama Çalışma Süresi (MET) ile analiz edilmiştir.

Anahtar Kelimeler: SEIR matematiksel modeli, Yapay Sinir Ağı hesaplaması, sürüleme teknikleri, SQP, Meksika Şapkası Dalga Dönüşümü.

1. INTRODUCTION

In recent years, mathematical models have been applied to solve and understand the dynamics of the models used to investigate the dynamics of the Zika virus [1], dengue virus [2], HIV [3], malaria [4], COVID-19 [5], and LD [6].

The Zika virus is an epidemic that can spread through the transmission of the virus known as Aedes. The symptoms of this virus are treacherous and it can spread within 3 to 14 days. The symptoms are low during the first few days which makes the virus dangerous. The virus can be controlled by using the treatment and the early forecasting of the virus. The Zika Virus was exposed in the middle of the last era [7]. The Zika epidemic disease has been exposed in Uganda. The major cause of the virus is the macaque which belongs to the Rhesus category [8].

* *Sorumlu Yazar (Corresponding Author)*
e-mail : junaid.ali@hitecuni.edu.pk

In contrast to the dengue virus, the Zika virus is more dangerous due to its prolonged presence in the human body, the duration of this virus is three days to two weeks whereas the dengue virus remains in the human body from 2 days to 1 week. No appropriate virus treatment has been invented to control the vector along with the insecticide spray and stop the larval breeding atmosphere. The major cause of the virus is the female macaque who is expecting. It designated the susceptible infected as per the circumstance. As the mathematical models are promising to deal with epidemic diseases, researchers proposed various mathematical models for the numerical treatment of the Zika virus [1, 7-17].

To understand the system's dynamics, these differential equations must be solved correctly. Several numerical solvers for the Zika virus mathematical model were created by researchers. [1, 7-17], however in classical approaches, the entire tedious process is carried out to obtain intermediate or floating value outcomes. Furthermore, approaches such as the Adomian family and other perturbation techniques diverge as the input domain grows larger, whereas the suggested scheme remains convergent. Classical methods are particularly prone to variable overwriting and overload. Unlike Stochastic Numerical Solvers (SNS), classical numerical and analytical solvers are not generalizable and so cannot be implemented on parallel architectures.

Stochastic numerical solvers with various hybridization optimization strategies aid in the solution of complex real-world applications such as climate modeling, bioinformatics, energy systems, chemistry, and epidemiology, all of which involve uncertainty, unpredictability, and many dynamics. The SNS combines the stochastic technique with hybrid optimization schemes to get consistent and trustworthy results.

The current study aims to develop a numerical solver for the nonlinear SEIR mathematical model of the Zika disease using efficient stochastic computing techniques by utilizing the Mexican hat wavelet feed-forward ANN. The optimization of the designed ANN is executed by utilizing the computing efficiency of PSO aided with efficient local optimizer SQP i.e. MHW-ANN-PSO-SQP. In the recent past various stochastic computing techniques have been applied to solve the nonlinear mathematical system for Zika disease. However, the MHW-ANN-PSO-SQP technique has never been applied to solve this nonlinear system. The mathematical formulation of SEIR Zika disease along with the parameters' details and values are presented in [1] and written in (1).

$$\begin{aligned}
&\frac{dS_h(y)}{dy} = A_h - S_h(y)\beta_h\left(I_v(y) + \rho I_h(y)\right) - \mu_h S_h(y), \quad (S_H)_0 = k_1,\\
&\frac{dE_H(y)}{dy} = \beta_H\left(\rho I_H(y) + I_V(y)\right)S_H(y) - (\chi_H + \mu_H)E_H(y), \quad (E_H)_0 = k_2,\\
&\frac{dI_H(y)}{dy} = \chi_H E_H(y) - (\eta + \mu_H + \gamma)I_H(y), \quad (I_H)_0 = k_3,\\
&\frac{dR_H(y)}{dy} = -\mu_H R_H(y) + \gamma I_H(y), \quad (R_H)_0 = k_4,\\
&\frac{dS_v(y)}{dy} = A_v - \beta_v I_H(y)S_v(y) - \mu_H S_v(y), \quad (S_v)_0 = k_5,\\
&\frac{dE_v(y)}{dy} = \beta_v I_H(y)S_v(y) - (\mu_v+\delta_H)E_v(y), \quad (E_v)_0 = k_6,\\
&\frac{dI_v(y)}{dy} = E_v(y)S\delta_v(y) - \mu_v I_v(y), \quad (I_v)_0 = k_7,
\end{aligned} \tag{1}$$

The list of parameters used in the above system along with the values are tabulated in Table 1. The use of the stochastic computing procedure to solve the various nonlinear coupled and non-coupled differential systems is common and promising, however, the Mexican hat wavelet-based ANN-PSO-SQP numerical solver has never been investigated for the numerical treatment nonlinear coupled model.

Currently, some of the applications of the stochastic computing procedure to solve infectious diseases like the COVID pandemic [18-27], hepatitis [28-30], breakbone fever [31-35], and influenza [36-38], and CD4+T HIV system [39]. The other applications for these solvers are the numerical treatment of predator model [40], Emden system [41, 42], film_flow system [43], mass and heat system [44], hydrothermal system [45], large scale system [46], Emden model [47], life Cycle Optimization [48], Flierl equations [49, 50], Singular Periodic [51], Predictive system[40, 52], Smoke nonlinear model [53], nervous stomach system [54], Engineering problems [55], Transport system[56], and the Love story of Layle [57]. stochastic computing procedure is hybridized with the global bio-inspired GA, Swarm PSO, and Ant Colony Optimization (ACO) along with local search scheme, SQP, SQM, ASM, and simulated annealing [46, 48, 50]. The ANN-based solvers used the Log sigmoid, Morlet Wavelet (MW), as an activation function [28, 29, 31, 40, 54, 58, 59].

While the ANN-based numerical solver GA-ASA lacks precision and incurs high computing costs, numerical solvers struggle with generalizability when addressing the Zika virus nonlinear differential model. Numerous applications have demonstrated the effectiveness of an ANN-based numerical solver that leverages the computational efficiency of Mexican hats wavelet and optimized PSO-SQP hybridization techniques, which can be a good candidate to solve the Zika virus more precisely and accurately at a low computing cost.

Some of the novelties of the proposed MHW-ANN-PSO-SQP are listed as follows:

- A swarm-based stochastic computing procedure, MHW-ANN-PSO-SQP, is presented for numerically treating the nonlinear coupled mathematical system of SEIR to model the dynamics of the Zika virus.
- The error-based fitness function is optimized through PSO and SQP i.e. PSO-SQP in a hybrid manner.
- The accuracy of the developed swarming computational procedure based on MHW is validated by comparing the obtained results with the reference solution and the ANN-GA-ASA solutions.
- The precision of the proposed scheme is tested through the small AE for the numerical treatment of a nonlinear SEIR based on the Zika virus.
- To validate the stability and reliability of the proposed MHW-ANN-PSO-SQP, comprehensive statistical analysis has been made through the Mean Square Error (MSE), Mean Absolute Deviation (MAD), Global Mean Square Error (GMSE), and Global Mean Absolute Deviation (GMAD).
- The computational complexity of the proposed scheme is analyzed through Mean Execution Time (MET).

The rest of the paper is summarized as follows: Section 2 discusses the methodology, optimization procedure, and statistical operators. Section 3 presents the simulation and result discussion, while the last section provides the conclusion and the future direction.

2. DESIGN METHODOLOGY

The current section deals with formulating an error-based fitness function, the hybridization procedure using swarm-based PSO along with SQP, and the construction of statistical operators.

2.1. Construction of Fitness Function

The mathematical presentation of the stochastic computing procedure i.e. MHW-ANN for the system presented in (1) can be written as:

$$\begin{aligned}
&\frac{d\tilde{S}_h(y)}{dy}, \frac{d\tilde{E}_h(y)}{dy}, \frac{d\tilde{I}_h(y)}{dy}, \frac{d\tilde{R}_h(y)}{dy}, \frac{d\tilde{S}_v(y)}{dy}, \frac{d\tilde{E}_v(y}{dy} \\
&= \left[\sum_{i=1}^{m} \alpha_{s_{h,i}} f\left(w_{s_{h,i}}(y)\right.\right. \\
&+ b_{s_{h,i}}\Big), \sum_{i=1}^{m} \alpha_{E_{h,i}} f(w_{I_{h,i}}(y) \\
&+ b_{E_{h,i}}), \sum_{i=1}^{m} \alpha_{I_{h,i}} f(w_{R_{h,i}}(y) \\
&+ b_{I_{h,i}}), \sum_{i=1}^{m} \alpha_{R_{h,i}} f(w_{R_{h,i}}(y) \\
&+ b_{R_{h,i}}), \sum_{i=1}^{m} \alpha_{S_{v,i}} f\left(w_{S_{v,i}}(y)\right. \\
&+ b_{S_{v,i}}\Big), \sum_{i=1}^{m} \alpha_{E_{v,i}} f(w_{E_{v,i}}(y) \\
&+ b_{E_{v,i}}), \sum_{i=1}^{m} \alpha_{I_{v,i}} f(w_{I_{r,i}}(y) + b_{I_{v,i}})\Big]
\end{aligned} \tag{2}$$

The study used the Mexican hat wavelet (MHW) as an activation function. The mathematical formulation of the MHW is presented in (3).

$$f(\tilde{y}) = \frac{2}{\sqrt{3}} \pi^{-\frac{1}{4}} (1 - y^2) e^{-\frac{y^2}{2}} \tag{3}$$

The MHW-based ANN formulation of the nonlinear coupled SEIR system based on Zika virus $\hat{S}_h(y), \hat{E}_h(y), \hat{I}_h(y), \hat{R}_h(y), \hat{S}_v(y), \hat{E}_v(y), \hat{I}_v(y)$ along with the derivative is:

$$\left[\frac{d\tilde{S}_h^{'}(y)}{dy},\frac{d\tilde{E}_h^{'}(y)}{dy},\frac{d\tilde{I}_h^{'}(y)}{dy},\frac{d\tilde{R}_h^{'}(y)}{dy},\frac{d\tilde{S}_v^{'}(y)}{dy},\frac{d\tilde{E}_v^{'}(y)}{dy},\frac{d\tilde{I}_v^{'}(y)}{dy}\right]$$
$$=\left[\sum_{k=1}^{m}\alpha\tilde{S}_h\left[\frac{2}{\sqrt{3}}\pi^{-0.25}(1-(w\tilde{S}_h(y)+b\tilde{S}_h)^2)e^{-0.5(w\tilde{S}_h+b\tilde{S}_h)^2}\right],\sum_{k=1}^{m}\alpha\tilde{E}_h\left[\frac{2}{\sqrt{3}}\pi^{-0.25}(1-(w\tilde{E}_h(y)+b\tilde{E}_h)^2)e^{-0.5(w\tilde{I}_h+b\tilde{I}_h)^2}\right],\sum_{k=1}^{m}\alpha\tilde{I}_h\left[\frac{2}{\sqrt{3}}\pi^{-0.25}(1-(w\tilde{I}_h(y)+b\tilde{I}_h)^2)e^{-0.5(w\tilde{I}_h+b\tilde{I}_h)^2}\right],\sum_{k=1}^{m}\alpha\tilde{R}_h\left[\frac{2}{\sqrt{3}}\pi^{-0.25}(1-(w\tilde{R}_h(y)+b\tilde{R}_h)^2)e^{-0.5(w\tilde{R}_h+b\tilde{R}_h)^2}\right],\sum_{k=1}^{m}\alpha\tilde{S}_v\left[\frac{2}{\sqrt{3}}\pi^{-0.25}(1-(w\tilde{S}_v(y)+b\tilde{S}_v)^2)e^{-0.5(w\tilde{S}_v+b\tilde{S}_v)^2}\right],\sum_{k=1}^{m}\alpha\tilde{E}_h\left[\frac{2}{\sqrt{3}}\pi^{-0.25}(1-(\tilde{E}_h(y)+b\tilde{E}_h)^2)e^{-0.5(w\tilde{E}_h+b\tilde{E}_h)^2}\right],\sum_{k=1}^{m}\alpha\tilde{I}_v\left[\frac{2}{\sqrt{3}}\pi^{-0.25}(1-(w\tilde{I}_h(y)+b\tilde{I}_v)^2)e^{-0.5(w\tilde{I}_v+b\tilde{I}_v)^2}\right]\right] \quad (4)$$

The unknown parameters of the proposed scheme can be presented as:

$$P=\begin{bmatrix}P_{\tilde{S}_h}\\P_{\tilde{E}_h}\\P_{\tilde{I}_h}\\P_{\tilde{R}_h}\\P_{\tilde{S}_v}\\P_{\tilde{E}_v}\\P_{\tilde{I}_v}\end{bmatrix}\text{ for }P_{\tilde{S}_h}=\begin{bmatrix}w_{\tilde{S}_h}\\\alpha_{\tilde{S}_h}\\b_{\tilde{S}_h}\end{bmatrix},P_{\tilde{E}_h}=\begin{bmatrix}w_{\tilde{E}_h}\\\alpha_{\tilde{E}_h}\\b_{\tilde{E}_h}\end{bmatrix},P_{\tilde{I}_h}=\begin{bmatrix}P_{\tilde{I}_h}\\\alpha_{\tilde{I}_h}\\b_{\tilde{I}_h}\end{bmatrix},$$
$$P_{\tilde{R}_h}=\begin{bmatrix}w_{\tilde{R}_h}\\\alpha_{\tilde{R}_h}\\b_{\tilde{R}_h}\end{bmatrix},P_{\tilde{S}_v}=\begin{bmatrix}w_{\tilde{S}_v}\\\alpha_{\tilde{S}_v}\\b_{\tilde{S}_v}\end{bmatrix},P_{\tilde{E}_v}=\begin{bmatrix}w_{\tilde{E}_v}\\\alpha_{\tilde{E}_v}\\b_{\tilde{E}_v}\end{bmatrix},P_{\tilde{I}_v}=\begin{bmatrix}w_{I_v}\\\alpha_{\tilde{I}_v}\\b_{\tilde{I}_v}\end{bmatrix}$$

The error based fitness function is as follow:

$$\epsilon_F=\epsilon_{\tilde{S}_h}+\epsilon_{\tilde{E}_h}+\epsilon_{\tilde{I}_h}+\epsilon_{\tilde{R}_h}+\epsilon_{\tilde{S}_v}+\epsilon_{\tilde{E}_v}+\epsilon_{\tilde{I}_v}+\epsilon$$

Error error-based fitness function of ϵ_F can be derived by the expressions given below:

$$\epsilon_{\tilde{S}_h}=\frac{1}{N}\sum_{i=1}^{N}\left[\frac{d\check{S}_H(y)}{dy}-A_H+\check{S}_H(y)\beta_H\left(\check{I}_v(y)-\rho\check{I}_H(y)\right)+\mu_H\check{S}_H(y)\right]^2$$
$$\epsilon_{\tilde{E}_h}=\frac{1}{N}\sum_{k=1}^{N}\left[\frac{d\check{E}_H(y)}{dy}-\beta_H\left(\rho\check{I}_H(y)-\check{I}_V(y)\right)\check{S}_H(y)+(\chi_H+\mu_H)\check{E}_H(y)\right]^2$$
$$\epsilon_{I_h}=\frac{1}{N}\sum_{k=1}^{N}\left[\frac{d\check{I}_H(y)}{dy}-\chi_H\check{E}_H(y)+(\eta+\mu_H+\gamma)\check{I}_H(y)\right]^2$$
$$\epsilon_{\tilde{R}_h}=\frac{1}{N}\sum_{k=1}^{N}\left[\frac{d\check{R}_H(y)}{dy}+\mu_H\check{R}_H(y)-\gamma\check{I}_H(y)\right]^2 \quad (5)$$
$$\epsilon_{\tilde{S}_v}=\frac{1}{N}\sum_{k=1}^{N}\left[\frac{d\check{S}_v(y)}{dy}-A_v+\beta_v\check{I}_H(y)\check{S}_v(y)+\mu_H\check{S}_v(y)\right]^2$$
$$\epsilon_{\tilde{E}_v}=\frac{1}{N}\sum_{k=1}^{N}\left[\frac{d\check{E}_v(y)}{dy}-\beta_v\check{I}_H(y)\check{S}_v(y)+(\mu_v+\delta_H)\check{E}_v(y)\right]^2$$
$$\epsilon_{\tilde{I}_v}=\frac{1}{N}\sum_{k=1}^{N}\left[\frac{d\check{I}_v(y)}{dy}-\check{E}_v(y)\check{S}\delta_v(y)+\mu_v\check{I}_v(y)\right]^2$$
$$\epsilon=\frac{1}{5}\left[\left(\tilde{S}_h(0)-k_1\right)^2+\left(\tilde{E}_h(0)-k_2\right)^2+\left(\tilde{I}_h(0)-k_3\right)^2+\left(\tilde{R}_h(0)-k_4\right)^2+\left(\tilde{S}_v(0)-k_5\right)^2+\left(\tilde{E}_v(0)-k_6\right)^2,(\tilde{I}_v(0)-k_7)^2\right]$$

$\check{S}_h(y),\check{E}_h(y),\check{I}_h(y),\check{R}_h(y),\check{S}_v(y),\check{E}_v(y),\check{I}_v(y)$ are the ANN-based outcomes for each class whereas the $\epsilon_{\tilde{S}_h},\epsilon_{\tilde{E}_h},\epsilon_{\tilde{I}_h},\epsilon_{\tilde{R}_h},\epsilon_{\tilde{S}_v},\epsilon_{\tilde{E}_v},\epsilon_{\tilde{I}_v}and\ \epsilon$ are error-based fitness functions. The fitness function ϵ is calculated through the initial conditions. Fig. 1 Shows the MHW-based ANN structure through global swarming (PSO)

and local search (SQP) procedure to solve the coupled nonlinear mathematical model of SEIR based on the Zika virus.

2.2. Optimization Procedure: PSO-SQP

This section provides the optimization technique for the numerical treatment of a nonlinear coupled system presented in (1) through MHW-ANN-PSO-SQP.

PSO is a swarm-based search algorithm that was presented during the last decade to solve global optimization problems. It is used to solve the constrained and unconstrained optimization problems using the global best approach. It works with the iterative process through local best and global best particles. It is the alternative global search technique of genetic algorithms. It is more efficient and has less computational cost. Some of the applications of the PSO are found in [18, 22, 38, 56, 60-64]. The PSO is upgraded by adding an effective local optimization scheme. The study used the local search SQP to get fast and accurate results by using the hybridization procedure with PSO. During the recent century, the SQP has been used in various applications [46, 48, 50, 65-67]. The Steps of the proposed PSO-SQP optimization algorithm is given in Algorithm 1. Parameters used in the proposed hybrid PSO-SQP along with the values can be found in [68].

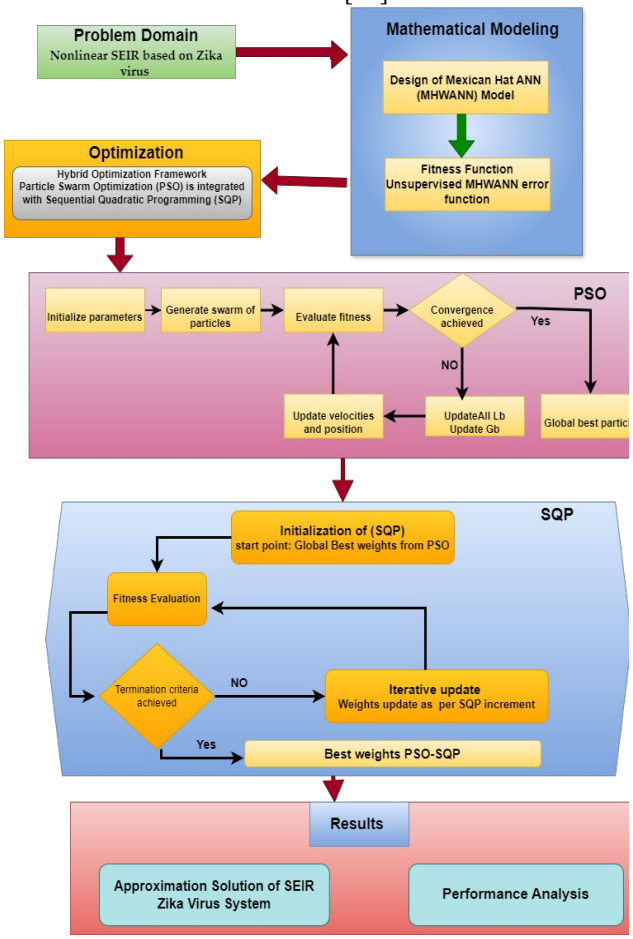

Figure 1. Workflow of the Proposed MHW-ANN-PSO-SQP for the Numerical Treatment of SEIR Coupled System Based on Zika Disease

Algorithm 1: Proposed Hybrid PSO-SQP

Optimization of PSO Technique

[Input]: The particles of the network are indicated in vector P.

[Population]: The illustration of the particle set is provided as $W = \begin{bmatrix} P_{\tilde{S}_h} \\ P_{\tilde{E}_h} \\ P_{\tilde{I}_h} \\ P_{\tilde{R}_h} \\ P_{\tilde{S}_v} \\ P_{\tilde{E}_v} \\ P_{\tilde{I}_v} \end{bmatrix}$

Where $P_{\tilde{S}_h} = \begin{bmatrix} w_{\tilde{S}_h} \\ \alpha_{\tilde{S}_h} \\ b_{\tilde{S}_h} \end{bmatrix}, P_{\tilde{E}_h} = \begin{bmatrix} w_{\tilde{E}_h} \\ \alpha_{\tilde{E}_h} \\ b_{\tilde{E}_h} \end{bmatrix}, P_{\tilde{I}_h} = \begin{bmatrix} P_{\tilde{I}_h} \\ \alpha_{\tilde{I}_h} \\ b_{\tilde{I}_h} \end{bmatrix}, P_{\tilde{R}_h} = \begin{bmatrix} w_{\tilde{R}_h} \\ \alpha_{\tilde{R}_h} \\ b_{\tilde{R}_h} \end{bmatrix}, P_{\tilde{S}_v} = \begin{bmatrix} w_{\tilde{S}_v} \\ \alpha_{\tilde{S}_v} \\ b_{\tilde{S}_v} \end{bmatrix}, P_{\tilde{E}_v} = \begin{bmatrix} w_{\tilde{E}_v} \\ \alpha_{\tilde{E}_v} \\ b_{\tilde{E}_v} \end{bmatrix}, P_{\tilde{I}_v} = \begin{bmatrix} w_{\tilde{I}_v} \\ \alpha_{\tilde{I}_v} \\ b_{\tilde{I}_v} \end{bmatrix}$

Where W, α, and b are the unknown variables of the network.

[Output]: Global Best vector $W_{\text{PSO-Best}}$

[Initialization]: For the given set of particles Specify the random values $M_{\text{PSO-Best}}$

[Fitness Evaluation]: Updated the fitness values of the variable ϵ_F using Eq. (6)

[Termination]: The algorithm will stop when the following conditions are met then store

1. Meet the fitness criteria. The algorithm converges and optimal fitness is achieved.
2. The algorithm reached the maximum iteration.

[Ranking]: Ranke the $W_{\text{PSO-Best}}$ in vector M. The vector contains the optimal values for the unknown variables.

[Storage]: Store the time, weights, function count, iterations

End of PSO Algorithm

Start of [SQP] procedure

Step a: Starting of SQP: the SQP is initialized using the MATLAB built-in function by using the best values generated by PSO along with the parameter's values. Details can be found in [68]
Step b: Calculation of Fitness of Knowns: Fitness values of Unknowns are calculated.
Step c: Termination of SQP: Terminate the recurrent process of SQP to update the weights of the unknowns of the developed PSO-SQP by using the conditions
The number of iterations reached
Maximum fitness values achieved
Step d: Adjust the weights of unknowns: Optimize the weights for each iteration.

End of SQP Algorithm

Generate $W_{PSO\text{-}SQP}$

2.3. Performance Operators

The accuracy of the designed scheme i.e. MHW-ANN-PSO-SQP is validated in various performance indicators. The mathematical formulation of the performance operators is written as follows.

$$\begin{aligned} absoulte\ error = & \sum_{i=1}^{n} \left|S_{h_i} - \check{S}_{h_i}\right|, \left|E_{h_i}\right. \\ & - \check{E}_{h_i}\left|, \left|I_{h_i} - \check{I}_{h_i}\right|, \left|R_{h_i}\right.\right. \\ & - \check{R}_{h_i}\left|, \left|S_{v_i} - \check{S}_{v_i}\right|, \left|E_{v_i}\right.\right. \\ & - \check{E}_{v_i}\left|, \left|I_{v_i} - \check{I}_{v_i}\right|\right. \end{aligned} \tag{6}$$

$$\begin{aligned} mean\ squre\ error = & \frac{1}{n}\sum_{i=1}^{n} (S_{h_i} \\ & - \check{S}_{h_i})^2, (E_{h_i} \\ & - \check{E}_{h_i})^2, (I_{h_i} \\ & - \check{I}_{h_i})^2, (R_{h_i} \\ & - \check{R}_{h_i})^2, (S_{v_i} \\ & - \check{S}_{v_i})^2, (E_{v_i} \\ & - \check{E}_{v_i})^2, (I_{v_i} - \check{I}_{v_i})^2 \end{aligned} \tag{7}$$

$$\begin{aligned} global\ mean\ squre\ error = & \sum_{i=1}^{100} \frac{1}{n}\sum_{i=1}^{n} (S_{h_i} \\ & - \check{S}_{h_i})^2, (E_{h_i} \\ & - \check{E}_{h_i})^2, (I_{h_i} \\ & - \check{I}_{h_i})^2, (R_{h_i} \\ & - \check{R}_{h_i})^2, (S_{v_i} \\ & - \check{S}_{v_i})^2, (E_{v_i} \\ & - \check{E}_{v_i})^2, (I_{v_i} - \check{I}_{v_i})^2 \end{aligned} \tag{8}$$

$$\begin{aligned} mean\ absoulte\ deviation = & \frac{1}{n}\sum_{i=1}^{n} \left|S_{h_i} - \check{S}_{h_i}\right|, \left|E_{h_i}\right. \\ & - \check{E}_{h_i}\left|, \left|I_{h_i} - \check{I}_{h_i}\right|, \left|R_{h_i}\right.\right. \\ & - \check{R}_{h_i}\left|, \left|S_{v_i} - \check{S}_{v_i}\right|, \left|E_{v_i}\right.\right. \\ & - \check{E}_{v_i}\left|, \left|I_{v_i} - \check{I}_{v_i}\right|\right. \end{aligned} \tag{9}$$

$$\begin{aligned} globale\ mean\ absoulte\ deviation = & \sum_{i=1}^{100} \frac{1}{n}\sum_{i=1}^{n} \left|S_{h_i}\right. \\ & - \check{S}_{h_i}\left|, \left|E_{h_i} - \check{E}_{h_i}\right|, \left|I_{h_i}\right.\right. \\ & - \check{I}_{h_i}\left|, \left|R_{h_i} - \check{R}_{h_i}\right|, \left|S_{v_i}\right.\right. \\ & - \check{S}_{v_i}\left|, \left|E_{v_i} - \check{E}_{v_i}\right|, \left|I_{v_i}\right.\right. \\ & - \check{I}_{v_i}\left|\right. \end{aligned} \tag{10}$$

$\check{S}_h(y), \check{E}_h(y), \check{I}_h(y), \check{R}_h(y), \check{S}_v(y)$, $\check{E}_v(y,)$ and $\check{I}_v(y)$ are the ANN-based solutions of SEIR mathematical model based on Zika virus. The study also analyzed the complexity of the proposed scheme through mean execution time.

3. NUMERICAL RESULTS

This section deals with the simulation and results discussion for the nonlinear mathematical SEIR system based on the Zika virus through the stochastic computing procedure along with the swarming approach which is aided by the local search scheme SQP. The best weights obtained by using the hybrid optimization procedure, evaluation of the solution, absolute error, statistical operators along complexity analysis have also been presented in this section.
The ANN-based numerical solution of the nonlinear coupled mathematical model based on the Zika virus is presented by using the suitable parameter values tabulated in Table 1 as follows:

$$\begin{aligned} & \frac{d\check{S}_H(y)}{dy} = (0.1) - \check{S}_H(y)(0.12)\left(\check{I}_v(y) + (0.14)\check{I}_H(y)\right) - (0.1)\check{S}_H(y), \quad (S_H)_0 = (0.10), \\ & \frac{d\check{E}_H(y)}{dy} = (0.12)\left((0.14)\check{I}_H(y) + \check{I}_V(y)\right)\check{S}_H(y) - \left((0.13) + (0.1)\right)\check{E}_H(y), \quad (E_H)_0 = (0.12), \end{aligned} \tag{11}$$

$$\frac{dI_H(y)}{dy} = (0.13)\check{E}_H(y) - \big((0.15) + (0.1) + (0.17)\big)\check{I}_H(y), \quad (I_H)_0 = (0.14),$$

$$\frac{d\check{R}_H(y)}{dy} = -(0.1)\check{R}_H(y) + (0.17)\check{I}_H(y), \quad (0.16),$$

$$\frac{d\check{S}_v(y)}{dy} = A_v - (0.2)\check{I}_H(y)\check{S}_v(y) - (0.1)\check{S}_v(y), \quad (S_v)_0 = (0.18),$$

$$\frac{d\check{E}_v(y)}{dy} = (0.2)\check{I}_H(y)\check{S}_v(y) - (0.3)+(0.22))\check{E}_v(y), \quad (0.20),$$

$$\frac{d\check{I}_v(y)}{dy} = \check{E}_v(y)(0.3)(y) - (0.3)\check{I}_v(y), = (0.22)$$

Table 1: List of parameters for SEIR based on Zika along with values

Parameter	Values	Parameter	Values
β_H	0.12	δ_V	0.3
A_H	0.1	μ_V	0.25
μ_H	0.1	k_1	0.10
χ_H	0.13	k_2	0.12
P	0.14	k_3	0.14
η	0.15	k_4	0.16
β_V	0.2	k_5	0.18
γ	0.17	kK_6	0.20
δ_H	0.22	K_7	0.22

The fitness function ϵ_F become

$$\epsilon_F = \frac{1}{N}\sum_{i=1}^{11}\Bigg[\Big[\frac{d\check{S}_H(y)}{dy} - (0.1) - \check{S}_H(y)(0.12)\Big(\check{I}_v(y) + (0.14)\check{I}_H(y)\Big) - (0.1)\check{S}_H(y)\Big]^2 + \Big[\frac{d\check{E}_H(y)}{dy} - (0.12)\Big((0.14)\check{I}_H(y) + \check{I}_V(y)\Big)\check{S}_H(y) - \big((0.13) + (0.1)\big)\check{E}_H(y)\Big]^2 + \Big[\frac{d\check{I}_H(y)}{dy} - (0.13)\check{I}_H(y) - \big((0.15) + (0.1) + (0.17)\big)\check{I}_H(y)\Big]^2 + \Big[\frac{d\check{R}_H(y)}{dy} - (0.1)\check{R}_H(y) + (0.17)\check{I}_H(y)\Big]^2 + \Big[\frac{d\check{S}_v(y)}{dy} - A_v - (0.2)\check{I}_H(y)\check{S}_v(y) - (0.1)\check{S}_v(y)\Big]^2 + \Big[\frac{d\check{E}_v(y)}{dy} - (0.2)\check{I}_H(y)\check{S}_v(y) - (0.3)+(0.22))\check{E}_v(y)\Big]^2 + \Big[\frac{d\check{I}_v(y)}{dy} - \check{E}_v(y)(0.3)(y) - (0.3)\check{I}_v(y)\Big]^2 \frac{1}{5}\Big[\big(\tilde{S}_h(0) - 0.10\big)^2 + \big(\tilde{E}_h(0) - 0.12\big)^2 + \big(\tilde{I}_h(0) - 0.14\big)^2 + \big(\tilde{R}_h(0) - 0.16\big)^2 + \big(\tilde{S}_v(0) - 0.18\big)^2 + \big(\tilde{E}_v(0) - 0.20\big)^2, \big(\tilde{I}_v(0) - 0.22\big)^2\Big]\Bigg] \quad (12)$$

For the numerical solution of the nonlinear SEIR mathematical system for the Zika disease, the fitness function presented in (11) has been optimized through a hybrid computing procedure i.e. PSO-SQP. For the statistical analysis, the 50 independent runs have been performed while 10 neurons i.e. 30 variables for each class. The optimal weights produced by the proposed hybrid PSO-SQP have been demonstrated in Fig. 2 (a-g). These weights are given to the system presented in (14) and used to optimize the fitness function.

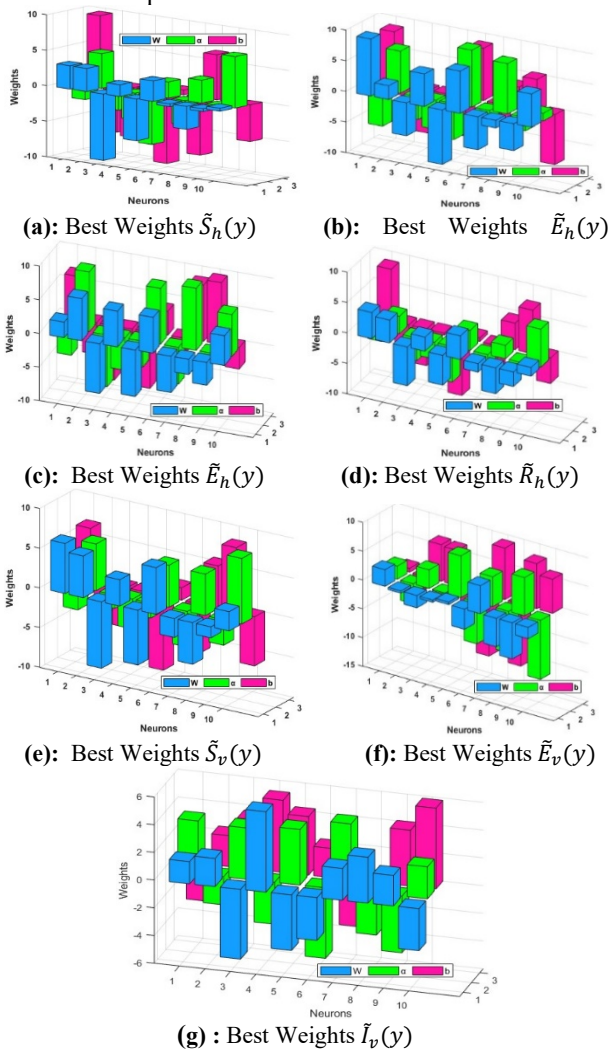

(a): Best Weights $\tilde{S}_h(y)$ **(b):** Best Weights $\tilde{E}_h(y)$

(c): Best Weights $\tilde{E}_h(y)$ **(d):** Best Weights $\tilde{R}_h(y)$

(e): Best Weights $\tilde{S}_v(y)$ **(f):** Best Weights $\tilde{E}_v(y)$

(g) : Best Weights $\tilde{I}_v(y)$

Figure 2. Best Weight vector for proposed PSO-NM for the non-linear mathematical SEIR System based on the Zika virüs

The study performs the comparative analysis of the outcome produced by the ANN-GA-ASA, RK numerical solvers, and the proposed stochastic computing procedure MHW-ANN-PSO-SQP through mean and best values. Fig 3 (a-g) shows the outcome for mean and best

values. The overlap solution validated the accuracy of the proposed scheme.

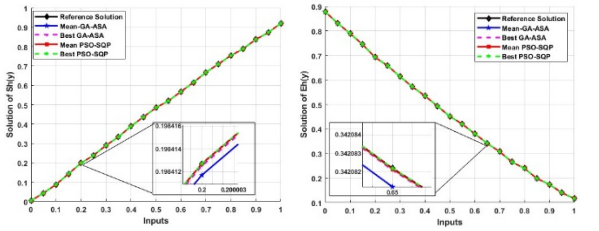

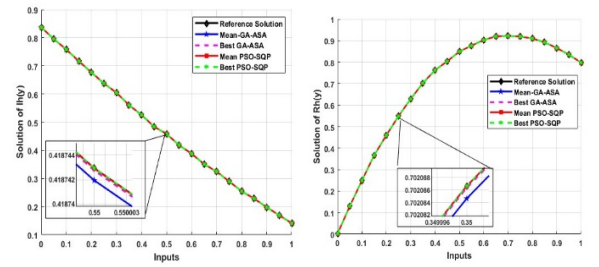

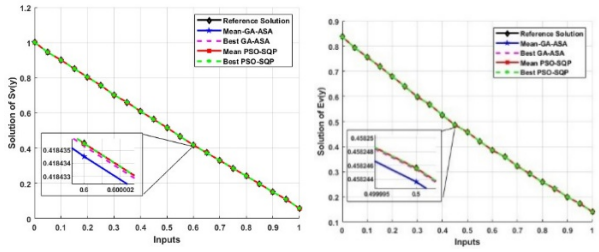

(e): Comparison of $\tilde{S}_v(y)$ **(f):** Comparison of $\tilde{E}_v(y)$

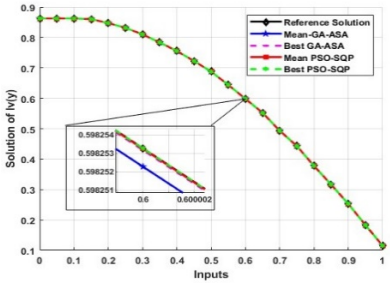

(g): Comparison of $\tilde{I}_v(y)$

Figure 3. (Cont.) Results compression of the Reference, ANN-GA-ASA, and Proposed MHW-ANN-PSO-SQP the non-linear mathematical SEIR System based on the Zika virus

To authenticate the precision of the proposed scheme, absolute error values through the mean and best are also performed. The results are plotted in Fig.4 (a-g) for ANNP-GA-ASA and Fig. 5(a-g) for the proposed MHW-ANN-PSO-SQP. One can observe that the AE of mean and best for ANNP-GA-SA are in the range 10^{-6} to 10^{-7}, while the AE for the developed procedure is between 10^{-8} to 10^{-9} respectively. The low AE measures confirm the precision of the developed scheme.

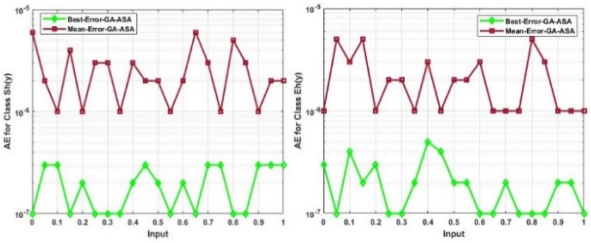

(a): AE for class $\tilde{S}_h(y)$ **(b):** AE for Class $\tilde{E}_h(y)$

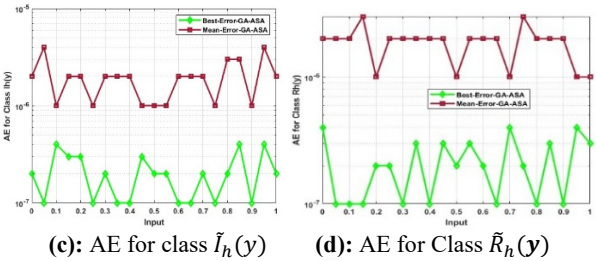

(c): AE for class $\tilde{I}_h(y)$ **(d):** AE for Class $\tilde{R}_h(y)$

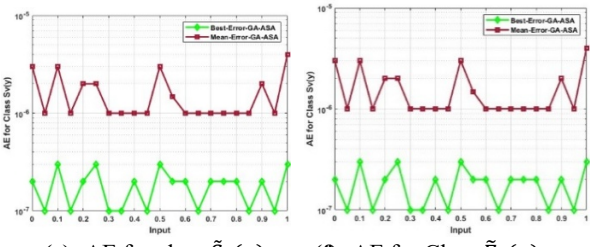

(e): AE for class $\tilde{S}_v(y)$ **(f):** AE for Class $\tilde{E}_v(y)$

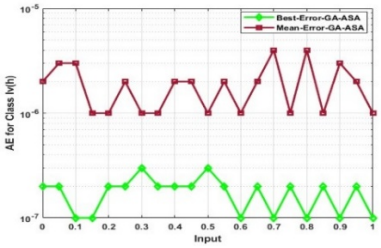

(g): AE for class $\tilde{I}_v(y)$

Figure 4. Best/Mean AE of ANN-GA-ASA of the non-linear SEIR System based on the Zika virüs

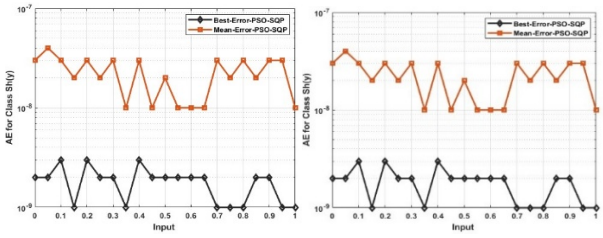

(a): AE for class $\tilde{S}_h(y)$ (b): AE for Class $\tilde{E}_h(y)$

Figure 5. Best/Mean AE of MHW-ANN-PSO-SQP for solving the system

To solve the nonlinear system of SEIR based on the Zika virus, the stability of the proposed scheme is examined through the statistical MSE and MAD operators. Results are demonstrated in Fig. 6(a-b). The MSE measures are in the range 10^{-07} to 10^{-12}, 10^{-07} to 10^{-12}, 10^{-07} to 10^{-12}, 10^{-07} to 10^{-13}, 10^{-07} to 10^{-12}, 10^{-07} to 10^{-13}, 10^{-07} to 10^{-13} respectively.

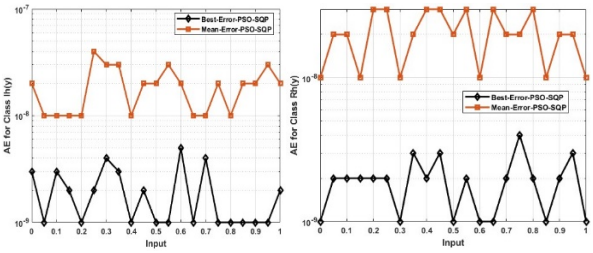

(c): AE for class $\tilde{I}_h(y)$ **(d):** AE for Class $\tilde{R}_h(y)$

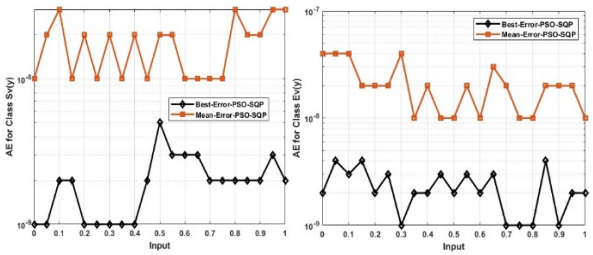

(e): AE for class $\tilde{S}_v(y)$ f): AE for Class $\tilde{E}_v(y)$

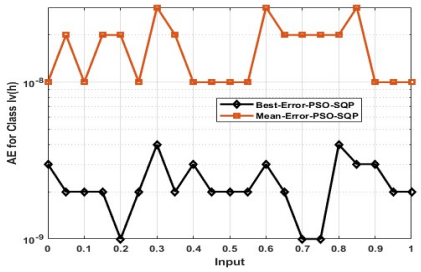

(g): AE for class $\tilde{I}_v(y)$

Figure 5. (Cont.) Best/Mean AE of MHW-ANN-PSO-SQP for solving the system

From the values, it is also observed that the values for MAD are in lie in the range 10^{-07} to 10^{-11}, 10^{-07} to 10^{-11}, 10^{-07} to 10^{-11}, 10^{-07} to 10^{-11}, 10^{-07} to 10^{-11}, 10^{-07} to 10^{-10}, 10^{-7} to 10^{-10}. The data is enlarged for fifty execution runs for the numerical treatment of the SEIR system. One can conclude that the accuracy in terms of MSE and MAD is almost same for the all trials, which confirms the stability of the proposed scheme. The statistical operator's measures for MSE and MAD to solve the SEIR mathematical system are presented in Fig. 7.

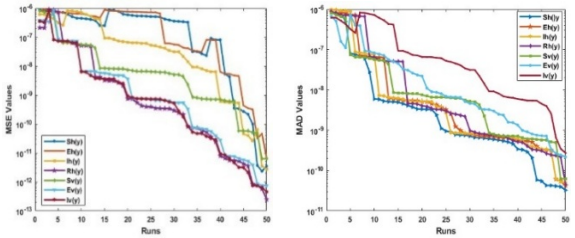

(a): MSE Measure **(b):** MAD Measure

Figure 6. MSE (a), MAD (b) Measure of the developed MHW-ANN-PSO-SQP

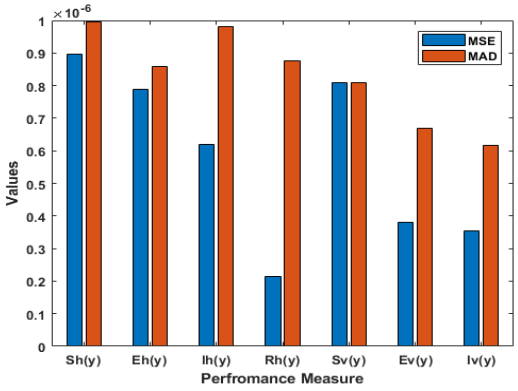

The accuracy of the developed swarm computing technique is further validated through the statistical operator's minimum (Min), mean, and Standard Deviation (std). The values are tabulated in Table 2-5. Table 2 presents the dynamics of $\tilde{S}_h(y)$ and $\tilde{E}_h(y)$. The min values that represent the best operators lie between 10^{-09} to 10^{-12} and 10^{-08} to 10^{-12} respectively, the values for mean and std are calculated as 10^{-06} to 10^{-07}, and 10^{-06} to 10^{-08} for class $\tilde{S}_h(y)$ and $\tilde{E}_h(y)$. Table 3 demonstrates the min, mean, and std operator measures for classes $\tilde{I}_h(y)$ and $\tilde{R}_h(y)$. The performance measures for the Min, mean and Std are in the range 10^{-09} to 10^{-11}, 10^{-08} to 10^{-12}, 10^{-07} to 10^{-08}, 10^{-07} to 10^{-08}, and 10^{-07} to 10^{-08}, 10^{-07} to 10^{-08} respectively. Table 4 tabulates the min, mean, and std operator measures for classes $\tilde{S}_v(y)$ and $\tilde{E}_v(y)$. The performance measures for the Min, mean and Std are in the range 10^{-07} to 10^{-11}, 10^{-07} to 10^{-08}, 10^{-6} to 10^{-08}, 10^{-08} to 10^{-11}, and 10^{-07} to 10^{-08}, 10^{-07} to 10^{-08} respectively. Moreover, Table 5 illustrates the min, mean, and std operator measures for classes $\tilde{I}_v(y)$. The performance measures for the Min, mean and Std are in the range 10^{-09} to 10^{-12}, 10^{-07} to 10^{-08}, and 10^{-6} to 10^{-8}.

Table 2: Statistical measure for classes $\tilde{S}_h(y)$, $\tilde{E}_h(y)$

y	Min	Mean	Std	Min	Mean	Std
	$\tilde{S}_h(y)$			$\tilde{E}_h(y)$		
0	3.55E-11	3.55E-08	5.55E-06	5.50E-09	5.50E-08	5.35E-07
0.05	4.31E-10	8.35E-08	2.33E-07	2.55E-09	3.55E-08	2.55E-07
0.1	3.52E-09	5.52E-07	5.20E-06	5.30E-10	5.35E-07	5.20E-06
0.15	6.46E-10	6.50E-07	6.25E-06	3.65E-09	2.50E-07	2.50E-06
0.2	4.66E-09	2.22E-08	5.35E-07	5.50E-10	5.20E-07	3.65E-06
0.25	3.83E-09	1.33E-07	9.50E-07	6.30E-09	3.35E-08	5.55E-06
0.3	5.55E-11	6.24E-07	5.20E-07	5.55E-10	2.40E-09	2.25E-06
0.35	3.65E-10	3.62E-07	6.65E-07	6.60E-09	6.75E-08	3.53E-07
0.4	4.64E-09	5.25E-07	3.45E-07	2.50E-09	5.35E-07	5.35E-07
0.45	9.52E-10	3.53E-08	5.50E-07	5.40E-10	2.55E-08	8.64E-06
0.5	3.22E-09	2.66E-07	2.35E-06	8.22E-09	3.22E-06	2.55E-07
0.55	4.56E-11	5.25E-08	4.20E-06	3.55E-10	8.30E-09	5.35E-07
0.6	6.33E-11	6.40E-07	3.55E-07	5.45E-09	2.74E-08	2.55E-08
0.65	2.79E-01	2.65E-07	2.65E-07	2.55E-10	3.55E-09	3.23E-07
0.7	3.64E-10	3.55E-08	5.50E-07	4.35E-09	5.23E-08	5.35E-07
0.75	8.53E-09	5.26E-07	3.35E-06	2.20E-09	6.40E-08	2.50E-07
0.8	5.65E-08	4.54E-07	5.40E-06	5.80E-09	4.55E-07	3.45E-06
0.85	3.22E-09	3.45E-08	5.55E-07	3.50E-08	5.30E-09	8.33E-07
0.9	6.63E-09	2.35E-07	3.25E-07	6.35E-09	3.45E-07	7.25E-07
0.95	2.94E-10	5.53E-08	5.50E-07	5.25E-08	5.55E-06	5.35E-07
1	6.33E-09	3.35E-08	6.30E-07	5.55E-08	6.35E-07	5.42E-07

Table 3: Statistical measure for classes $\tilde{I}_h(y)$, $\tilde{R}_h(y)$

y	Min	Mean	Std	Min	Mean	Std
	$\tilde{S}_v(y$			$\tilde{E}_v(y)$		
0	5.55E-09	5.35E-08	5.58E-07	5.35E-09	5.55E-07	3.25E-07
0.05	2.23E-07	3.55E-08	5.30E-06	3.54E-11	2.34E-08	5.55E-07
0.1	3.40E-11	2.65E-07	2.53E-07	2.65E-10	5.23E-08	4.50E-08
0.15	4.35E-08	4.22E-07	3.55E-07	5.20E-08	5.55E-07	5.35E-07
0.2	2.55E-09	5.53E-07	5.84E-06	2.65E-09	2.45E-07	4.43E-07
0.25	5.20E-10	2.40E-07	4.33E-07	3.55E-07	2.30E-08	2.55E-06
0.3	3.55E-08	3.30E-08	3.25E-07	2.35E-08	3.55E-07	3.55E-07
0.35	2.35E-10	5.20E-07	6.45E-07	5.53E-09	4.25E-08	5.40E-07
0.4	5.55E-09	4.55E-08	5.64E-08	3.50E-11	5.50E-08	9.32E-06
0.45	5.52E-12	3.55E-07	8.33E-06	5.44E-08	2.35E-07	3.55E-06
0.5	3.54E-09	5.65E-07	5.95E-07	2.85E-10	3.25E-07	2.55E-06
0.55	2.35E-09	4.25E-09	2.50E-07	8.50E-05	5.50E-07	4.25E-07
0.6	4.20E-09	3.30E-08	6.76E-07	3.35E-11	2.55E-07	6.55E-07
0.65	5.55E-08	5.55E-07	3.30E-07	4.55E-09	5.35E-07	3.40E-07
0.7	9.33E-10	4.44E-08	4.64E-08	6.53E-10	3.55E-08	4.55E-07
0.75	3.54E-10	6.55E-07	6.56E-07	5.75E-08	5.54E-08	2.30E-06
0.8	5.20E-09	5.33E-07	3.54E-07	4.25E-09	4.45E-07	3.55E-06
0.85	2.55E-11	8.55E-07	9.60E-06	3.57E-10	2.55E-07	5.55E-07
0.9	5.25E-09	5.23E-08	5.35E-08	5.30E-12	3.35E-07	4.25E-07
0.95	3.35E-09	3.50E-08	3.55E-07	2.55E-09	5.52E-07	6.55E-07
1	5.55E-09	2.50E-07	5.55E-07	2.55E-09	5.55E-07	8.55E-07

Table 4: Statistical measure for classes $\tilde{S}_v(y)$, $\tilde{E}_v(y)$

y	Min	Mean	Std	Min	Mean	Std
	$\tilde{S}_v(y$			$\tilde{E}_v(y)$		
0	5.55E-09	5.35E-08	5.58E-07	5.35E-09	5.55E-07	3.25E-07
0.05	2.23E-07	3.55E-08	5.30E-06	3.54E-11	2.34E-08	5.55E-07
0.1	3.40E-11	2.65E-07	2.53E-07	2.65E-10	5.23E-08	4.50E-08
0.15	4.35E-08	4.22E-07	3.55E-07	5.20E-08	5.55E-07	5.35E-07
0.2	2.55E-09	5.53E-07	5.84E-06	2.65E-09	2.45E-07	4.43E-07
0.25	5.20E-10	2.40E-07	4.33E-07	3.55E-07	2.30E-08	2.55E-06
0.3	3.55E-08	3.30E-08	3.25E-07	2.35E-08	3.55E-07	3.55E-07
0.35	2.35E-10	5.20E-07	6.45E-07	5.53E-09	4.25E-08	5.40E-07
0.4	5.55E-09	4.55E-08	5.64E-08	3.50E-11	5.50E-08	9.32E-06
0.45	5.52E-12	3.55E-07	8.33E-06	5.44E-08	2.35E-07	3.55E-06
0.5	3.54E-09	5.65E-07	5.95E-07	2.85E-10	3.25E-07	2.55E-06
0.55	2.35E-09	4.25E-09	2.50E-07	8.50E-05	5.50E-07	4.25E-07
0.6	4.20E-09	3.30E-08	6.76E-07	3.35E-11	2.55E-07	6.55E-07
0.65	5.55E-08	5.55E-07	3.30E-07	4.55E-09	5.35E-07	3.40E-07
0.7	9.33E-10	4.44E-08	4.64E-08	6.53E-10	3.55E-08	4.55E-07
0.75	3.54E-10	6.55E-07	6.56E-07	5.75E-08	5.54E-08	2.30E-06
0.8	5.20E-09	5.33E-07	3.54E-07	4.25E-09	4.45E-07	3.55E-06
0.85	2.55E-11	8.55E-07	9.60E-06	3.57E-10	2.55E-07	5.55E-07
0.9	5.25E-09	5.23E-08	5.35E-08	5.30E-12	3.35E-07	4.25E-07
0.95	3.35E-09	3.50E-08	3.55E-07	2.55E-09	5.52E-07	6.55E-07
1	5.55E-09	2.50E-07	5.55E-07	2.55E-09	5.55E-07	8.55E-07

Table 5: Statistical measure for class $\tilde{I}_v(y)$

y	Min	Mean	Std
	$\tilde{I}_v(y)$		
0	4.55E-09	2.55E-07	4.50E-07
0.05	3.40E-09	5.42E-07	2.35E-06
0.1	2.55E-09	5.35E-08	3.50E-08
0.15	5.35E-08	3.55E-07	5.25E-07
0.2	5.53E-10	5.55E-07	2.50E-06
0.25	4.55E-08	4.23E-07	3.55E-07
0.3	3.40E-09	5.20E-08	5.35E-07
0.35	5.40E-09	2.45E-07	2.23E-07
0.4	6.35E-09	2.55E-08	5.55E-08
0.45	5.25E-12	5.30E-08	4.55E-06
0.5	3.50E-09	3.45E-08	3.24E-06
0.55	2.20E-10	5.50E-08	2.55E-07
0.6	6.50E-09	2.22E-07	5.30E-07
0.65	8.55E-09	4.34E-07	6.26E-07
0.7	5.23E-10	5.85E-07	4.55E-06
0.75	3.55E-09	5.20E-07	3.60E-07
0.8	5.34E-09	3.32E-07	2.55E-07
0.85	2.25E-11	2.55E-07	6.20E-07
0.9	4.52E-09	5.20E-07	2.60E-06
0.95	6.50E-10	3.53E-07	5.46E-07
1	5.25E-10	2.52E-07	5.35E-07

Table 6: Comparative Analysis of the Proposed Scheme with ADM and GA-ASA.

Class	AE			MSE			MAD		
	ADM	GA-ASA	**Proposed**	ADM	GA-ASA	**Proposed**	ADM	GA-ASA	**Proposed**
$\tilde{S}_h(y)$	10^{-4}	10^{-7}	$\mathbf{10^{-8}}$	10^{-5}	10^{-9}	$\mathbf{10^{-11}}$	10^{-4}	10^{-8}	$\mathbf{10^{-11}}$
$\tilde{E}_h(y)$	10^{-4}	10^{-7}	$\mathbf{10^{-8}}$	10^{-5}	10^{-9}	$\mathbf{10^{-11}}$	10^{-4}	10^{-8}	$\mathbf{10^{-11}}$
$\tilde{I}_h(y)$	10^{-3}	10^{-6}	$\mathbf{10^{-8}}$	10^{-5}	10^{-9}	$\mathbf{10^{-12}}$	10^{-4}	10^{-7}	$\mathbf{10^{-10}}$
$\tilde{R}_h(y)$	10^{-4}	10^{-7}	$\mathbf{10^{-9}}$	10^{-6}	10^{-10}	$\mathbf{10^{-13}}$	10^{-4}	10^{-7}	$\mathbf{10^{-10}}$
$\tilde{S}_v(y)$	10^{-3}	10^{-7}	$\mathbf{10^{-8}}$	10^{-5}	10^{-8}	$\mathbf{10^{-12}}$	10^{-5}	10^{-7}	$\mathbf{10^{-10}}$
$\tilde{E}_v(y)$	10^{-4}	10^{-8}	$\mathbf{10^{-9}}$	10^{-5}	10^{-9}	$\mathbf{10^{-12}}$	10^{-4}	10^{-7}	$\mathbf{10^{-11}}$
$\tilde{I}_v(y)$	10^{-4}	10^{-7}	$\mathbf{10^{-9}}$	10^{-5}	10^{-8}	$\mathbf{10^{-12}}$	10^{-4}	10^{-8}	$\mathbf{10^{-10}}$

Table 7: Assessment of the Reliability of the proposed MHW-ANN-PSO-SQP

Class	Method	GMSE		GMAD	
		Values	**STD**	**Values**	**STD**
$\tilde{S}_h(y)$	GA-ASA	3.234E-09	6.432E-09	8.315E-09	8.264E-08
	PSO-SQP	**3.318E-11**	**3.821E-11**	**2.638E-10**	**2.425E-09**
$\tilde{E}_h(y)$	GA-ASA	4.378E-09	2.734E-09	5.942E-08	6.342E-08
	PSO-SQP	**2.321E-12**	**6.354E-10**	**6.248E-09**	**5.916E-09**
$\tilde{I}_h(y)$	GA-ASA	5.348E-09	4.328E-09	3.727E-08	2.538E-08
	PSO-SQP	**6.934E-11**	**7.981E-09**	**5.326E-09**	**6.382E-09**
$\tilde{R}_h(y)$	GA-ASA	8.453E-09	3.642E-09	2.984E-08	3.824E-08
	PSO-SQP	**2.546E-11**	**4.528E-10**	**8.328E-09**	**5.255E-09**
$\tilde{S}_v(y)$	GA-ASA	5.842E-09	5.438E-08	3.237E-08	2.562E-08
	PSO-SQP	**6.438E-11**	**7.327E-10**	**8.547E-10**	**8.623E-09**
$\tilde{E}_v(y)$	GA-ASA	3.328E-09	3.439E-08	2.983E-08	5.177E-08
	PSO-SQP	**7.746E-11**	**9.984E-10**	**6.327E-10**	**5.734E-09**
$\tilde{I}_v(y)$	GA-ASA	3.743E-09	2.324E-09	3.921E-08	3.243E-08
	PSO-SQP	**2.954E-12**	**5.457E-11**	**6.457E-10**	**4.325E-09**

Table 6 shows the comparison of the proposed approach with ADM techniques and the ANN-based solver. The findings show that the proposed approach works better to solve the nonlinear SEIR system based on the propagation of the Zika virus.

The reliability of the developed MHW-ANN-PSO-SQP is testified using the global operators i.e. GMSE and GMAD through 100 runs. The mathematical formulation of the global statistical operations is presented in (9,11). The values tabulated in Table 7 indicate the developed procedure is consistent and stable.

The values for the proposed scheme are in the range 10^{-11} to 10^{-12}, and 10^{-10} the low values are the indication for the precision and accuracy of the scheme. The values for ANN-GA-ASA are in the range 10^{-09} and 10^{-09}.

The execution time of the proposed scheme is further analyzed through mean execution time. It is clear from the results, that the proposed scheme is computationally expensive. This is due to the hybridization of PSO and SQP. However, the designed scheme is accurate and precise in solving the nonlinear mathematical SEIR system based on the Zika virus. The mean execution time of the proposed scheme is 20 minutes while the mean execution of the ANN-GA-ASA [69] is 22.5 minutes. The values for mean execution time are shown in Figure 8. All the simulation is performed on an HP Folio notebook with SSD and 16GB RAM.

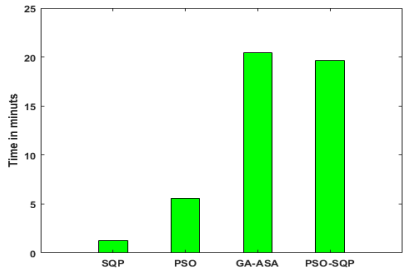

Figure 8. Mean Execution Time (MET) in minutes

4. CONCLUSION

The numerical treatment for the solution of the nonlinear mathematical SEIR model based on the Zika virus has been presented in the current study. The computational efficiency of MHW-based feed-forward artificial neural network, swarming optimization technique based on global particle swarm optimization, and local search sequential quadratic programming have been utilized to solve the SEIR system based on the Zika virus. The mathematical model of the Zika virus is based on the SEIR-coupled nonlinear system. The error-based fitness function based on SEIR differential equations is constructed through MHW-ANN-PSO-SQP in an unsupervised manner. The solution obtained through the proposed MHW-ANN-PSO-SQP is compared with the ANN-GA-ASA and numerical RK method. The overlap solutions designate the correctness of the proposed scheme, and the precision of the proposed scheme is testified through AE. It is found that the AE lies in the range 10^{-8} to 10^{-9}, additionally, the stability, convergence, and reliability are evaluated through detailed statistical analysis. The results indicated that the proposed scheme is stable, convergent, and reliable for solving the SEIR mathematical model based on the Zika virus. The proposed scheme is computationally efficient as compared to the scheme presented in [69].

In forthcoming studies, the proposed MHW-PSO-SQP can be applied to solve the coupled differential system based on a computer virus, COVID-19 system, fluid systems, and higher-order differential equations.

DECLARATION OF ETHICAL STANDARDS

The author(s) of this article declare that the materials and methods used in this study do not require ethical committee permission and/or legal-special permission.

AUTHORS' CONTRIBUTIONS

Farhad Muhammad RİAZ: Performing the experiments analyzing the results, and writing the manuscript.

Junaid Ali KHAN: Performing the experiments analyzing the results, and writing the manuscript.

CONFLICT OF INTEREST

There is no conflict of interest in this study.

REFERENCES

[1] S. Suantai, Z. Sabir, M. A. Z. Raja, and W. Cholamjiak, "Numerical Computation of SEIR Model for the Zika Virus Spreading," ***Cmc-Computers Materials & Continua,*** no. 1, vol. 75, pp. 2155-2170, (2023).

[2] Y. M. Rangkuti, S. Side, and M. S. M. Noorani, "Numerical analytic solution of SIR model of dengue fever disease in south Sulawesi using homotopy perturbation method and variational iteration method," ***Journal of Mathematical and Fundamental Sciences,*** no. 1, vol. 46, pp. 91-105, (2014).

[3] D. E. Kirschner, "" Dynamics of HIV Infection of CD4+ T cells," *SMR,* vol. 780, p. 18, (1993).

[4] K. S. Nisar, M. W. Anjum, M. A. Z. Raja, and M. Shoaib, "Design of a novel intelligent computing framework for predictive solutions of malaria propagation model,**" *Plos one,* no. 4, vol. 19, p. e0298451, (2024).

[5] I. Cooper, A. Mondal, and C. G. Antonopoulos, "A SIR model assumption for the spread of COVID-19 in different communities," ***Chaos, Solitons & Fractals,*** vol. 139, p. 110057, (2020).

[6] M. F. Khan *et al.*, "A new fractional model for vector-host disease with saturated treatment function via singular and non-singular operators," ***Alexandria Engineering Journal,*** no. 1, vol. 60, pp. 629-645, (2021).

[7] D. I. Simpson, "Zika virus infection in man," ***Transactions of the Royal Society of Tropical Medicine and Hygiene,*** no. 4, vol. 58, pp. 335-8, (1964).

[8] A. A. Al-Qahtani, N. Nazir, M. R. Al-Anazi, S. Rubino, and M. N. Al-Ahdal, "Zika virus: a new pandemic threat," ***The Journal of Infection in Developing Countries,*** no. 03, vol. 10, pp. 201-207, (2016).

[9] E. Bonyah and K. O. Okosun, "Mathematical modeling of Zika virus," ***Asian Pacific Journal of Tropical Disease,*** no. 9, vol. 6, pp. 673-679, (2016).

[10] F. Agusto, S. Bewick, and W. Fagan, "Mathematical model for Zika virus dynamics with sexual transmission route," ***Ecological Complexity,*** vol. 29, pp. 61-81, (2017).

[11] F. B. Agusto, S. Bewick, and W. Fagan, "Mathematical model of Zika virus with vertical transmission," ***Infectious Disease Modelling,*** no. 2, vol. 2, pp. 244-267, (2017).

[12] A. Wiratsudakul, P. Suparit, and C. Modchang, "Dynamics of Zika virus outbreaks: an overview of mathematical modeling approaches," ***PeerJ,*** vol. 6, p. e4526, (2018).

[13] S. Rezapour, H. Mohammadi, and A. Jajarmi, "A new mathematical model for Zika virus transmission," ***Advances in difference equations,*** no. 1, vol. 2020, pp. 1-15, (2020).

[14] A. Ali, Q. Iqbal, J. K. K. Asamoah, and S. Islam, "Mathematical modeling for the transmission potential of Zika virus with optimal control strategies," ***The European Physical Journal Plus,*** no. 1, vol. 137, p. 146, (2022).

[15] S. A. Jose *et al.*, "Mathematical modeling on co-infection: transmission dynamics of Zika virus and Dengue fever," ***Nonlinear Dynamics,*** no. 5, vol. 111, pp. 4879-4914, (2023).

[16] S. K. Biswas, U. Ghosh, and S. Sarkar, "A mathematical model of Zika virus transmission with saturated incidence and optimal control: A case study of 2016 zika outbreak in Puerto Rico," ***International Journal of Modelling and Simulation,*** no. 3, vol. 44, pp. 172-189, (2024).

[17] L. Wang, Q. Jia, G. Zhu, G. Ou, and T. Tang, "Transmission dynamics of Zika virus with multiple infection routes and a case study in Brazil," ***Scientific Reports,*** no. 1, vol. 14, p. 7424, (2024).

[18] S. Suantai, Z. Sabir, M. A. Z. Raja, and W. Cholamjiak, "Swarming Computational Procedures for the Coronavirus-Based Mathematical SEIR-NDC Model," ***Journal of Mathematics,*** vol. 2022, (2022).

[19] Z. Sabir, M. A. Z. Raja, S. E. Alhazmi, M. Gupta, A. Arbi, and I. A. Baba, "Applications of artificial neural network to solve the nonlinear COVID-19 mathematical model based on the dynamics of SIQ," ***Journal of Taibah University for Science,*** no. 1, vol. 16, pp. 874-884, (2022).

[20] M. Umar, Z. Sabir, M. A. Z. Raja, M. Shoaib, M. Gupta, and Y. G. Sánchez, "A stochastic intelligent computing with neuro-evolution heuristics for nonlinear SITR system of novel COVID-19 dynamics," ***Symmetry,*** no. 10, vol. 12, p. 1628, (2020).

[21] M. Umar *et al.*, "Numerical investigations through ANNs for solving COVID-19 model," ***International Journal of Environmental Research and Public Health,*** no. 22, vol. 18, p. 12192, (2021).

[22] M. Umar, Z. Sabir, M. A. Z. Raja, F. Amin, T. Saeed, and Y. Guerrero-Sanchez, "Integrated neuro-swarm heuristic with interior-point for nonlinear SITR model for dynamics of novel COVID-19," ***Alexandria Engineering Journal,*** no. 3, vol. 60, pp. 2811-2824, (2021).

[23] Y. G. Sánchez, Z. Sabir, and J. L. Guirao, "Design of a nonlinear SITR fractal model based on the dynamics of a novel coronavirus (COVID-19)," ***Fractals,*** no. 08, vol. 28, p. 2040026, (2020).

[24] Z. Sabir, M. A. Z. Raja, H. M. Baskonus, and A. Ciancio, "Numerical performance using the neural networks to solve the nonlinear biological quarantined based COVID-19 model," ***Atti della Accademia Peloritana dei Pericolanti-Classe di Scienze Fisiche, Matematiche e Naturali,*** no. 1, vol. 1, p. 10, (2023).

[25] A. Elsonbaty, Z. Sabir, R. Ramaswamy, and W. Adel, "Dynamical analysis of a novel discrete fractional SITRS model for COVID-19," ***Fracta ls,*** no. 08, vol. 29,p. 2140035, (2021).

[26] T. Botmart, Z. Sabir, S. Javeed, R. A. S. Núñez, M. R. Ali, and R. Sadat, "Artificial neural network-based heuristic to solve COVID-19 model including government strategies and individual responses," ***Informatics in Medicine Unlocked,*** vol. 32, p. 101028, (2022).

[27] A. N. Akkilic, Z. Sabir, M. A. Z. Raja, and H. Bulut, "Numerical treatment on the new fractional-order SIDARTHE COVID-19 pandemic differential model via neural networks," ***The European Physical Journal Plus,*** no. 3, vol. 137, p. 334, (2022).

[28] M. Umar, Z. Sabir, M. A. Z. Raja, H. M. Baskonus, S.-W. Yao, and E. Ilhan, "A novel study of Morlet neural networks to solve the nonlinear HIV infection system of latently infected cells," ***Results in Physics,*** vol. 25, p. 104235, (2021).

[29] Z. Sabir, M. Umar, M. A. Z. Raja, H. M. Baskonus, and W. Gao, "Designing of Morlet wavelet as a neural network for a novel prevention category in the HIV system," ***International Journal of Biomathematics,*** no. 04, vol. 15, p. 2250012, (2022).

[30] Z. Sabir, M. Umar, M. A. Z. Raja, and D. Baleanu, "Numerical solutions of a novel designed prevention class in the HIV nonlinear model "***CMES-Computer Modeling in Engineering & Sciences,*** no. 1,129, (2021).

[31] M. Umar, Z. Sabir, M. A. Zahoor Raja, K. Al-Basyouni, S. Mahmoud, and Y. G. Sánchez, "An advance computing numerical heuristic of nonlinear SIR dengue fever system using the Morlet wavelet kernel," ***Journal of Healthcare Engineering,*** vol. 2022, 1, (2022).

[32] M. Umar, Z. Sabir, M. A. Z. Raja, and Y. G. Sánchez, "A stochastic numerical computing heuristic of SIR nonlinear model based on dengue fever," ***Results in Physics,*** vol. 19, p. 103585, (2020).

[33] M. Umar, Kusen, M. A. Z. Raja, Z. Sabir, and Q. Al-Mdallal, "A computational framework to solve the nonlinear dengue fever SIR system," *Computer Methods in Biomechanics and Biomedical Engineering,* no. 16, vol. 25, pp. 1821-1834, (2022).

[34] Z. Sabir, M. A. Z. Raja, S. Javeed, and Y. G.-S. Nchez, "Numerical investigations of a fractional nonlinear dengue model using artificial neural networks," ***Fractals (fractals),*** no. 10, vol. 30, pp. 1-12, (2022).

[35] P. Junsawang *et al.*, "Numerical simulations of vaccination and Wolbachia on dengue transmission dynamics in the nonlinear model," ***IEEE Access,*** vol. 10, pp. 31116-31144, (2022).

[36] Z. Sabir, S. B. Said, and Q. Al-Mdallal, "A fractional order numerical study for the influenza disease mathematical model," ***Alexandria Engineering Journal,*** vol. 65, pp. 615-626, (2023).

[37] Z. Sabir *et al.*, "Artificial neural network scheme to solve the nonlinear influenza disease model," ***Biomedical Signal Processing and Control,*** vol. 75, p. 103594, (2022).

[38] S. Noinang *et al.*, "Swarming Computational Techniques for the Influenza Disease System," ***Cmc-Computers Materials & Continua,*** no. 3, vol. 73, pp. 4851-4868, (2022).

[39] F. M. Riaz, S. Ahmad, J. A. Khan, S. Altaf, Z. ur Rehman, and S. K. Memon, "Numerical Treatment of Non-Linear System for Latently Infected CD4+ T Cells: A Swarm-Optimized Neural Network Approach," ***IEEE Access,*** *(*2024).

[40] M. Umar, Z. Sabir, M. A. Z. Raja, F. Amin, T. Saeed, and Y. G. Sanchez, "Design of intelligent computing solver with Morlet wavelet neural networks for nonlinear predator-prey model," ***Applied Soft Computing,*** vol. 134, p. 109975, (2023).

[41] Z. Sabir, M. A. Z. Raja, M. R. Ali, and R. Sadat, "An advanced computational intelligent approach to solve the third kind of nonlinear pantograph Lane–Emden differential system," ***Evolving Systems,*** pp. 1-20, (2022).

[42] W. Adel, Z. Sabir, H. Rezazadeh, and A. Aldurayhim, "Application of a Novel Collocation Approach for Simulating a Class of Nonlinear Third-Order Lane–Emden Model," ***Mathematical Problems in Engineering,*** vol. 2022, (2022).

[43] M. A. Z. Raja, J. A. Khan, and T. Haroon, "Stochastic numerical treatment for thin film flow of third-grade fluid using unsupervised neural networks," ***Journal of the Taiwan Institute of Chemical Engineers,*** vol. 48, pp. 26-39, (2015).

[44] T. Botmart, Z. Sabir, M. A. Z. Raja, R. Sadat, and M. R. Ali, "Stochastic procedures to solve the nonlinear mass and heat transfer model of Williamson nanofluid past over a stretching sheet," ***Annals of Nuclear Energy,*** vol. 181, p. 109564, (2023).

[45] F. Chaudhry, M. Amin, M. Iqbal, R. Khan, and J. A. Khan, "A novel chaotic differential evolution hybridized with quadratic programming for short-term hydrothermal

coordination," ***Neural Computing and Applications,*** vol. 30, pp. 3533-3544, (2018).

[46] A. J. Joshy, R. Dunn, M. Sperry, V. E. Gandarillas, and J. T. Hwang, "An SQP algorithm based on a hybrid architecture for accelerating optimization of large-scale systems," in ***Aiaa Aviation 2023 Forum***, p. 4263, (2023).

[47] J. A. Khan, M. A. Z. Raja, M. M. Rashidi, M. I. Syam, and A. M. Wazwaz, "Nature-inspired computing approach for solving non-linear singular Emden–Fowler problem arising in electromagnetic theory," ***Connection Science,*** vol. 27, no. 4, pp. 377-396, (2015).

[48] Q. Nguyen, M. Onur, and F. O. Alpak, "Nonlinearly Constrained Life-Cycle Production Optimization Using Sequential Quadratic Programming (SQP) With Stochastic Simplex Approximated Gradients (StoSAG)," in ***SPE Reservoir Simulation Conference***, : SPE, p. D011S002R001, (2023).

[49] M. A. Z. Raja, J. A. Khan, A. Zameer, N. A. Khan, and M. A. Manzar, "Numerical treatment of nonlinear singular Flierl–Petviashivili systems using neural networks models," ***Neural Computing and Applications,*** vol. 31, pp. 2371-2394, (2019).

[50] M. A. Z. Raja, J. A. Khan, N. I. Chaudhary, and E. Shivanian, "Reliable numerical treatment of nonlinear singular Flierl–Petviashivili equations for unbounded domain using ANN, GAs, and SQP," ***Applied Soft Computing,*** vol. 38, pp. 617-636, (2016).

[51] Z. Sabir, D. Baleanu, M. R. Ali, and R. Sadat, "A novel computing stochastic algorithm to solve the nonlinear singular periodic boundary value problems," *International Journal of Computer Mathematics,* no. 10, vol. 99, pp. 2091-2104, (2022).

[52] Z. Sabir, T. Botmart, M. A. Z. Raja, and W. Weera, "An advanced computing scheme for the numerical investigations of an infection-based fractional-order nonlinear prey-predator system," ***Plos one,*** no. 3, vol. 17, p. e0265064, (2022).

[53] Z. Sabir, M. A. Z. Raja, A. S. Alnahdi, M. B. Jeelani, and M. Abdelkawy, "Numerical investigations of the nonlinear smoke model using the Gudermannian neural networks," ***Math. Biosci. Eng,*** no. 1, vol. 19, pp. 351-370, (2022).

[54] Z. Sabir *et al.*, "A novel design of morlet wavelet to solve the dynamics of nervous stomach nonlinear model," ***International Journal of Computational Intelligence Systems,*** no. 1, vol. 15, p. 4, (2022).

[55] Z. Sabir, M. A. Z. Raja, M. Shoaib, R. Sadat, and M. R. Ali, "A novel design of a sixth-order nonlinear modeling for solving engineering phenomena based on neuro intelligence algorithm," ***Engineering with Computers,*** pp. 1-16, (2022).

[56] Z. Sabir, T. Saeed, J. L. Guirao, J. M. Sánchez, and A. Valverde, "A Swarming Meyer Wavelet Computing Approach to Solve the Transport System of Goods," ***Axioms,*** no. 5, vol. 12, p. 456, (2023).

[57] Z. Sabir and S. B. Said, "A fractional order nonlinear model of the love story of Layla and Majnun," ***Scientific Reports,*** no. 1, vol. 13, p. 5402, (2023).

[58] Z. Sabir, D. Baleanu, M. A. Z. Raja, A. S. Alshomrani, and E. Hincal, "Computational Performances of Morlet Wavelet Neural Network for Solving a Nonlinear Dynamic Based on the Mathematical Model of the Affection of Layla and Majnun," ***Fractals,*** no. 02, vol. 31, p. 2340016, (2023).

[59] Z. Masood, K. Majeed, R. Samar, and M. A. Z. Raja, "Design of Mexican Hat Wavelet neural networks for solving Bratu type nonlinear systems," ***Neurocomputing,*** vol. 221, pp. 1-14, (2017).

[60] A. G. Gad, "Particle swarm optimization algorithm and its applications: a systematic review," ***Archives of computational methods in engineering,*** no. 5, vol. 29, pp. 2531-2561, (2022).

[61] M. Jain, V. Saihjpal, N. Singh, and S. B. Singh, "An overview of variants and advancements of PSO algorithm," ***Applied Sciences,*** no. 17, vol. 12, p. 8392, (2022).

[62] E. Garcia-Gonzalo and J. L. Fernandez-Martinez, "A brief historical review of particle swarm optimization (PSO)," ***Journal of Bioinformatics and Intelligent Control,*** no. 1, vol. 1, pp. 3-16, (2012).

[63] S. G. Andrab, A. Hekmat, and Z. B. Yusop, "A review: evolutionary computations (GA and PSO) in geotechnical engineering," ***Computational Water, Energy, and Environmental Engineering,*** no. 2, vol. 6, pp. 154-179, (2017).

[64] J. J. Liang, A. K. Qin, P. N. Suganthan, and S. Baskar, "Comprehensive learning particle swarm optimizer for global optimization of multimodal functions," ***IEEE Transactions on evolutionary computation,*** no. 3, vol. 10, pp. 281-295, (2006).

[65] S. H. E. A. Aleem, A. F. Zobaa, and M. M. A. Aziz, "Optimal $ C $-type passive filter based on minimization of the voltage harmonic distortion for nonlinear loads," ***IEEE Transactions on Industrial Electronics,*** no. 1, vol. 59, pp. 281-289, (2011).

[66] S. Sivasubramani and K. Swarup, "Sequential quadratic programming based differential evolution algorithm for optimal power flow problem," ***IET generation, transmission & distribution,*** no. 11, vol. 5, pp. 1149-1154, (2011).

[67] J. Nocedal and S. J. Wright, ***Numerical optimization.*** **Springer**, (1999).

[68] M. A. Z. Raja, "Solution of the one-dimensional Bratu equation arising in the fuel ignition model using ANN optimised with PSO and SQP," ***Connection Science,*** no. 3, vol. 26, pp. 195-214, (2014).

[69] Z. Sabir, S. A. Bhat, M. A. Z. Raja, and S. E. Alhazmi, "A swarming neural network computing approach to solve the Zika virus model," ***Engineering Applications of Artificial Intelligence,*** vol. 126, p. 106924, (2023).